European Spine Journal (2024) 33:3315–3323
https://doi.org/10.1007/s00586-024-08419-y

REVIEW ARTICLE

Notochordal cell derived lesions: a 55-year casuistic analysis of 50 cases with radiologic-pathologic correlation in a tertiary referral hospital, and literature review

Eva Manuela Pena-Burgos[1] · Nerea Torena Lerchundi[2] · Jorge Fuentes-Sánchez[3] · Mar Tapia-Viñe[2] · Nicomedes Fernández-Baíllo[3] · Jose Juan Pozo-Kreilinger[1]

Received: 22 March 2024 / Revised: 17 June 2024 / Accepted: 16 July 2024 / Published online: 24 July 2024

Abstract

Distinct lesions are derived from notochordal cells (NCDL), ranging from benign to malignant ones. This study presents fifty NCDL cases diagnosed in a tertiary hospital of reference from the past 55 years: forty-two conventional chordomas, including one chondroid chordoma subtype, four benign notochordal cell tumors (BNCT), two conventional chordomas with BNCT foci, and two dedifferentiated chordomas. All patients were adults. Three BNCT were incidentally diagnosed, and one case presented local pain. Chordomas began with local pain and/or neurological symptoms. BNCT were well-defined intraosseous lesions, hypointense on T1-weighted images (WI) and hyperintense on T2-WI, without enhancement in the contrast. Conventional chordomas, including its chondroid subtype, were lobulated masses with cortical disruption and soft tissue extension, hypointense on T1-WI and hyperintense on T2-WI, with variable contrast enhancement. BNCT were histologically composed of solid sheets of vacuolated cells with clear cytoplasm and round and central nuclei. No atypia, lobular growth pattern, myxoid matrix, or bone infiltration were seen. Conventional chordomas were histologically composed of physaliphorous cells in a myxoid stroma with lobulated and infiltrating growth patterns. Observational follow-up using radiological controls was decided on for the BNCT cases. None of these cases presented local recurrence or metastasis. En-bloc resection and adjuvant radiotherapy were selected for sacral and vertebral chordoma cases. Sixteen patients died due to tumor-related factors; twenty-eight presented local recurrence, and four developed distant metastases. New therapeutic options are being studied for chordoma cases. Clinical, radiological, and histopathological data are necessary to properly diagnose and follow up of NCDL.

Keywords Notochordal cell derived lesions · Chordoma · Chondroid chordoma · Dedifferentiated chordoma · Benign notochordal cell tumor

Introduction

There are different notochordal cell derived lesions (NCDL) [1]. Benign notochordal cell tumor (BNCT) is a benign entity [2]. Chordoma is a primary osseous malignant and locally aggressive tumour [3] that account approximately 1% of all primary malignant bone tumors [4]. A new entity has been proposed, the atypical notochordal cell tumour [5], but some authors argue that its diagnostic criteria are ill defined [1]. Sometimes there are overlapping clinical, radiological and histopathological characteristics among these entities [6–8]. Rare extraskeletal chordomas [9] or extraskeletal BNCT have been reported [10]. Our aim is to review the clinical, radiological, and histopathological

✉ Eva Manuela Pena-Burgos
evapenaburgos.ep@gmail.com

[1] Pathology Department, La Paz University Hospital, Paseo de la Castellana, 261, Madrid 28046, Spain

[2] Radiology Department, La Paz University Hospital, Madrid, Spain

[3] Orthopaedic Surgery and Traumatology Department, La Paz University Hospital, Madrid, Spain

features, and the management of NCDL of a tertiary referral hospital.

Materials and methods

All the NCDL cases diagnosed in the Pathology Department at La Paz University Hospital in Madrid between 1966 and 2023 were retrospectively reviewed in the present study. Clinical and radiological information were obtained from the medical records. All available material from the pathology files was reviewed, including hematoxylin and eosin stains, and immunohistochemical studies. Patient epidemiological characteristics (sex, age), clinical aspects (pain, relapses, suspected diagnosis), location, radiological findings (growth, soft tissue invasion), macroscopic appearance, histopathological features, immunohistochemical profile, local recurrence, metastases development and treatment were analyzed. Ethics committee approval was not required in this retrospective observational study.

Results

Fifty cases of NCDL were found. The main characteristics of the cases are summarized in the table (Table 1), including forty-two conventional chordomas (one chondroid chordoma), four BNCT (one of them has been previously reported [13]), two conventional chordomas with BNCT foci, and two dedifferentiated chordomas. Representative cases are shown in the figures (Figs. 1, 2, 3, 4, 5 and 6). No poorly differentiated chordomas or extraskeletal tumors (either benign or malignant) were diagnosed. The average age at the time of diagnosis was 50 years (P25 = 40, P75 = 59). Twenty-eight patients were males and twenty-two were females. BNCT were diagnosed in adults aged 23, 29, 34 and 50 years. BNCT with chordoma were diagnosed in adults aged 35 and 77 years. Chondroid chordoma was diagnosed in a 41-year-old male and dedifferentiated chordomas in a 44-year-old female and a 66-year-old male. Fifteen chordomas appeared in the sacrum, twelve in the clivus, seven in the cervical vertebrae, six in the lumbar vertebrae, and one in a thoracic vertebra. BNCT and chordomas with BNCT foci cases appeared in the sacrum. The chondroid chordoma was found in the clival area and the dedifferentiated chordomas in a cervical vertebrae and sacrum.

Clinical presentation was variable in chordoma cases. Locoregional pain was observed in nineteen cases, paresthesia appeared in five patients, headache in three cases, diplopia in three cases, hearing loss in three patients, micturition incontinence in two cases, and motor loss in three cases. The thoracic vertebral chordoma case was incidentally detected in a radiological image. One of the BNCT patients experienced initial sacral pain with normal neurological exploration, and the other three BNCT cases were incidentally detected in radiological images obtained for other reasons.

Simple radiography of chordoma cases was available in sixteen cases. Fifteen chordomas revealed lytic lesions, five of which displayed extension into adjacent soft tissue; and one case revealed a sclerotic aspect. CT was available in twenty-two chordoma of our series. A lytic lesion was present in twenty-one cases; with extension into adjacent tissues in all of them. The other case was a sclerotic mass with cortical erosion and soft tissue invasion. MRI was available in thirty cases. A lobulated heterogeneous mass with soft tissue invasion was generally observed. They were isointense or hypointense on T1-weighted images (WI) and hyperintense on T2-WI and short inversion T1 recovery (STIR) images. Hypointense areas were seen in some cases. They revealed homogeneous contrast enhancement with gadolinium. The two chordomas with BNCT foci cases displayed findings similar to those of the conventional chordoma cases. CT and MRI were performed in all BNCT cases. BNCT were difficult to identify on CT, with only a very subtle sclerosis appearing. Well-defined and lobulated masses were observed in the MRI. They were hypointense or isointense to muscle on T1-WI and hyperintense on T2-WI and STIR images. They did not present contrast gadolinium enhancement. Cortical erosion or soft tissue invasion did not appear in any case. In the chondroid chordoma, a predominantly hyperintense heterogeneous mass with hypointense areas on T2-WI was seen. It displayed homogeneous contrast enhancement with gadolinium. In dedifferentiated chordomas, initial radiological images presented the conventional chordoma findings, although the posterior dedifferentiated component revealed a polylobulated, ill-defined solid mass that was isointense on T1-WI and hyperintense on T2-WI, with heterogeneous gadolinium enhancement.

The diagnosis was based on a core needle biopsy in thirty-three cases, including all of the BNCT, and in curettage tissue fragments of fifteen cases, including the chondroid chordoma. All of the cases were discussed in the Bone and Soft Tissue Tumors Committee. An observational follow-up based on annual MRI radiological controls was established for the BNCT cases. Surgical management or chordomas depended on the level affected, tumor characteristics, and patient comorbidities. In our series, there were a total of thirty surgically treated patients at the axial level. The intervention type, with either partial or radical resection of the affected vertebra, is presented in the table. Six chordoma patients were not candidates for surgery. Intensity-modulated radiation therapy (IMRT) was administered in thirty chordoma cases and proton therapy was used in three cases. They were administered after surgery or as single tratment.

Table 1 Demographic and clinical characteristics, treatment and follow-up of the cases

Case	Diagnosis	Age, sex	Tumor location	Clinical presentation	Treatment	Follow-up
1	BNCT	23, F	Sacrum	Incidentally detected	Observational follow-up	9 years, NED
2	BNCT	29, F	Sacrum	Incidentally detected	Observational follow-up	5 years, NED
3	BNCT	34, M	Sacrum	Pain, normal neurological exploration	Observational follow-up	2 years, NED
4	BNCT	50, F	Sacrum	Incidentally detected	Observational follow-up	9 years, NED
5	Conventional chordoma + BNCT	35, F	Sacrum	Local pain	IMRT + S2 partial resection level	4 years, local recurrence, death
6	Conventional chordoma + BNCT	77, M	Sacrum	INA	IMRT	3 years, NED
7	Conventional chordoma	38, M	Clivus	Paresthesia	Partial resection	34 years, local recurrence
8	Conventional chordoma	45, F	Clivus	Local pain	IMRT	7 years, local recurrence
9	Conventional chordoma	55, F	Clivus	Headache, hearing loss	Partial resection	INA
10	Conventional chordoma	60 F	Clivus	Paresthesia	IMRT + partial resection	13 years, local recurrence, death
11	Conventional chordoma	61, M	Clivus	Local pain, diplopia	IMRT	INA
12	Conventional chordoma	49, F	Clivus	Headache	IMRT	INA
13	Conventional chordoma	38, M	Clivus	Paresthesia, hearing loss	IMRT + partial resection	14 years, local recurrence death
14	Conventional chordoma	62, M	Clivus	Diplopia	Partial resection	15 years, NED
15	Conventional chordoma	72, M	Clivus	INA	IMRT + partial resection	INA
16	Conventional chordoma	48, F	Clivus	Local pain, headache	IMRT	17 years, local recurrence, death
17	Conventional chordoma	51, F	Clivus	INA	Partial resection	INA
18	Conventional chordoma	53, F	Clivus	Hearing loss	IMRT	28 years, local recurrence, lung metastases, death
19	Conventional chordoma	54, M	Cervical vertebra	Local pain	Partial resection	22 years, NED
20	Conventional chordoma	43, M	Cervical vertebra	INA	IMRT + Partial resection	INA
21	Conventional chordoma	67, F	Cervical vertebra	Paresthesia	Partial resection	13 years, local recurrence
22	Conventional chordoma	71, F	Cervical vertebra	Local pain	IMRT + partial resection	INA
23	Conventional chordoma	45, M	Cervical vertebra	INA	Partial resection	INA
24	Conventional chordoma	48, F	Cervical vertebra	Local pain	Partial resection	15 years, lung metastases, death
25	Conventional chordoma	55, M	Cervical vertebra	INA	IMRT + partial resection	INA
26	Conventional chordoma	51, M	Thoracic vertebra	Incidentally detected	Radical resection	4 years, NED
27	Conventional chordoma	62, F	Lumbar vertebra	INA	IMRT	INA
28	Conventional chordoma	38, F	Lumbar vertebra	Local pain	IMRT	10 years, local recurrence, death
29	Conventional chordoma	44, M	Lumbar vertebra	Local pain	Partial resection	49 years, local recurrence
30	Conventional chordoma	48, F	Lumbar vertebra	INA	IMRT	INA
31	Conventional chordoma	62, F	Lumbar vertebra	Local pain	IMRT + radical resection	21 years, local recurrence, death
32	Conventional chordoma	58, M	Lumbar vertebra	INA	IMRT	16 years, local recurrence, death
33	Conventional chordoma	54, M	Sacrum	Local pain, motor loss	IMRT + S2 partial resection level	INA
34	Conventional chordoma	60, F	Sacrum	Local pain	S3 partial resection level	5 years, NED
35	Conventional chordoma	52, F	Sacrum	Motor loss	IMRT	INA
36	Conventional chordoma	50, F	Sacrum	INA	IMRT + S2 partial resection level	12 years, NED
37	Conventional chordoma	36, M	Sacrum	Motor loss	IMRT	INA
38	Conventional chordoma	42, F	Sacrum	Local pain	Proton therapy + S3 partial resection level	2 years, NED
39	Conventional chordoma	46, F	Sacrum	Micturition incontinence	S2 partial resection level	9 years, local recurrence, death

Table 1 (continued)

Case	Diagnosis	Age, sex	Tumor location	Clinical presentation	Treatment	Follow-up
40	Conventional chordoma	48, M	Sacrum	INA	IMRT + Radical and reconstruction	INA
41	Conventional chordoma	53, F	Sacrum	Local pain	IMRT	17 years, local recurrence death
42	Conventional chordoma	56, F	Sacrum	Local pain	Proton therapy + S2 partial resection level	5 years, NED
43	Conventional chordoma	43, M	Sacrum	Micturition incontinence	IMRT + S1 resection and reconstruction	17 years, liver metastases, death
44	Conventional chordoma	47, F	Sacrum	Paresthesia	IMRT	INA
45	Conventional chordoma	60, M	Sacrum	Local pain	Proton therapy + S2 partial resection level	3 years, NED
46	Conventional chordoma	59, F	Sacrum	Local pain	IMRT + S3 partial resection level	INA
47	Conventional chordoma	53, M	Sacrum	INA	IMRT + S2 partial resection level	7 years, local recurrence, death
48	Chondroid chordoma	41, M	Clivus	Diplopia	Partial resection	14 years, death
49	Dedifferentiated chordoma	44, F	Cervical vertebra	Local pain	IMRT	21 years, local recurrence, death
50	Dedifferentiated chordoma	66, M	Sacrum	Local pain	IMRT	2 years, local recurrence, liver metastases, death

BNTC = benign notochordal cell tumor; M = male; F = female; IMRT = intensity-modulated radiation therapy; INA = information not available; NED = no evidence of disease

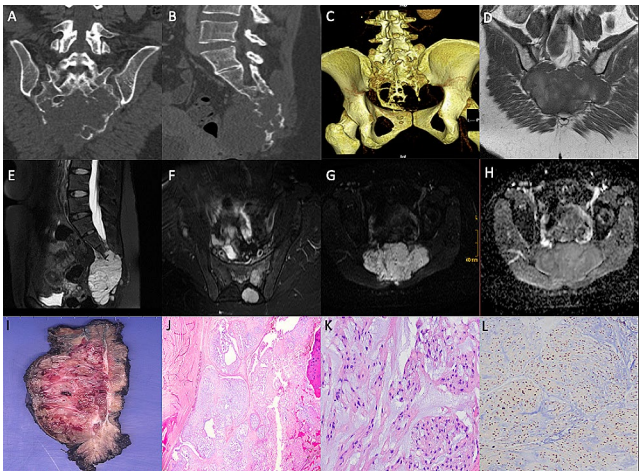

Fig. 1 Conventional sacral chordoma. Coronal non-contrast CT and B. Sagittal non-contrast CT: extensive lobulated-edged soft tissue mass centered on the sacrum which erodes and destroys it. C. Posterior VR reconstruction: sacral bone erosion. D. Axial T1: Lobulated and well-defined mass, isointense to the muscle and areas of increased signal that may be related to hemorrhage. E. Sagittal STIR sequence: relatively homogeneous signal. F. Axial STIR sequence: it invades the pelvic S2 foramen and extends to the articular surface with no apparent invasion of the sacroiliac space. G. Axial diffusion-weighted imaging and H. ADC Map: the tumor shows slight diffusion restriction. I. Sagittal gross section: sacrum destroyed and infiltrated by a polylobed tumor, with pelvic soft tissues invasion. J. Bone infiltrating tumor with lobulated growth pattern, fibrous septa, and myxoid matrix (H&E, x100). K. Cords of rounded and eosinophilic cells in a myxoid matrix (H&E, x400). L. Diffuse nuclear Brachyury positivity (x40)

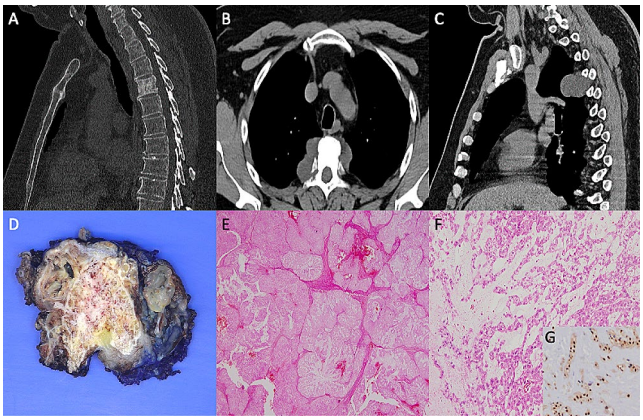

Fig. 2 Conventional vertebral chordoma. (**A**) Sagittal non-contrast CT: sclerotic involvement of the T4 vertebral body associated with irregularity and erosion of its posterior cortex. (**B**) Axial CT and (**C**) Sagittal non contrast CT: soft tissue mass that invades the medullary canal with an opening to the conjunctival foramina. (**D**) Axial gross section: heterogeneous lobulated mass with gelatinous matrix and soft tissue extension. (**E**) Lobulated growth pattern arranged in nests with myxoid matrix and separated by fibrous septa (H&E, x100). (**F**) Cords of physaliphorous cells (H&E, x200). (**G**) Diffuse nuclear Brachyury positivity (x400)

The surgical resected specimens were received and analyzed in the Pathology Department. Chordomas consisted mainly of infiltrating polylobed masses with solid, cystic, gelatinous, and hemorrhagic areas. In general, chordoma cases consisted of a bone-infiltrating tumor with a lobulated growth pattern separated by fibrous septa. Myxoid matrix was predominant but fibrous stroma areas were also seen. Cells were arranged in cords or nests. Polygonal cells

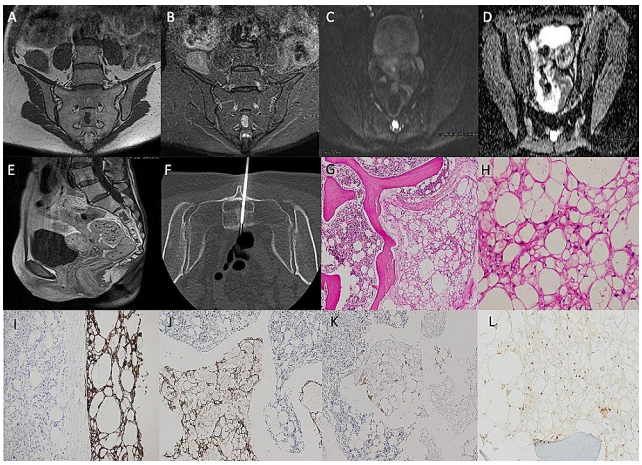

Fig. 3 BNCT. (**A**) Coronal T1: S2 central sacral isointense mass respect to the muscle with well-defined borders and lobulated margins. (**B**) Coronal long TR sequence FATSAT: the mass is hyperintense. (**C**) Coronal diffusion-weighted imaging and (**D**) Coronal ADC Map: the lesion facilitates diffusion. (**E**) Sagittal T1 after gadolinium: the lesion does not show enhancement. (**F**) Axial non-contrast CT: guided biopsy procedure. (**G**) Solid sheet of vacuolated cells with clear cytoplasm. Adjacent thickened and sclerotic preexisting bone trabecula (H&E, x100). (**H**) Cells with clear vacuolated cytoplasm and round and eccentric nuclei. (**I**) AE1/AE3 diffuse positivity (x100). (**J**) Diffuse positive S-100 (x100). **K**. EMA patchy positivity (x100). **L**. Diffuse nuclear Brachyury positivity (x200)

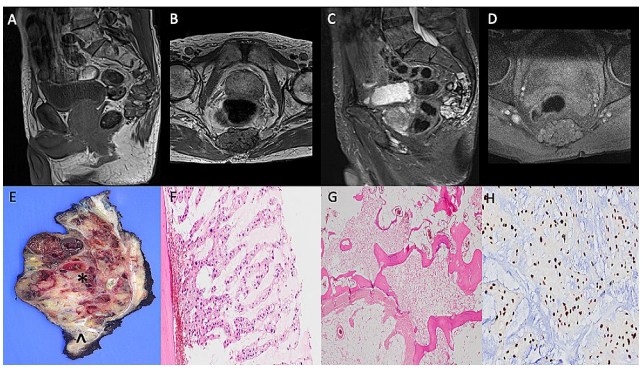

Fig. 4 BNCT and chordoma. (**A**) Sagittal non contrast T1: heterogeneous lesion, predominantly hypointense with isolated hyperintense foci, with lobed and well-defined contours centered from S3 to second coccygeal vertebral. (**B**) Axial T1: associates soft tissue mass that occupies presacral fat, without invasion of the rectum. (**C**) Sagittal long TR sequence: the mass is hyperintense. (**D**) Axial MRI with gadolinium: discrete homogeneous enhancement after gadolinium administration. (**E**) Sagittal gross section: lobulated tumor with abundant cystic areas (*), some with haematic material and others with gelatinous material; and solid areas (^); which extends to presacral soft tissues. (**F**) Cystic areas: Solid sheet of physaliphorous cells in a clear stroma (H&E, x200). (**G**) Solid areas: Solid sheet of vacuolated cells with clear cytoplasm and round and central nuclei adjacent to non-tumoral adipose tissue (H&E, x40). (**H**) Diffuse nuclear Brachyury positivity (x200)

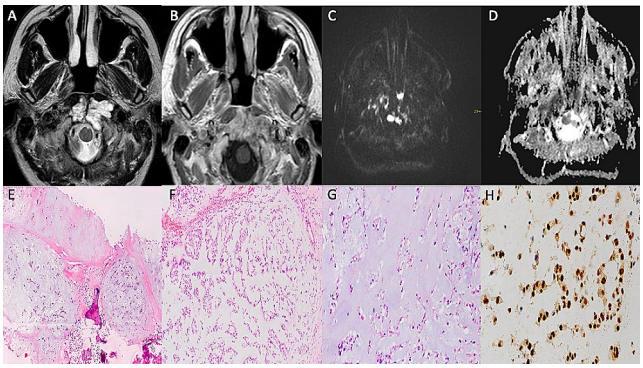

Fig. 5 Chondroid chordoma. (**A**) Axial T2-WI: hyperintense mass with some hypointense linear areas in the sphenoid bone base and C1 anterior arch with soft tissue associated component in paravertebral space and above the upper end of the odontoid process. (**B**) Axial MRI T1, post contrast: homogeneous enhancement. Axial diffusion map; and **D**. Axial ADC map: the mass show diffusion restriction. **E**. Lobulated infiltrating mass with chondroid matrix (H&E, x100). **F**. Chords of polygonal cells in a chondroid matrix (H&E, x100). **G**. Polygonal cells with eosinophilic cytoplasm (H&E, x200). **H**. Diffuse nuclear Brachyury positivity (x400)

with vacuolated cytoplasm and prominent central nucleus without visible nucleolus (physaliphorous cells) or more rounded and eosinophilic cells were observed. The chondroid chordoma showed a lobulated infiltrating mass made up of polygonal cell chords with eosinophilic cytoplasm in a hyaline chondroid matrix. The BNCT cases were histologically similar. They consisted of a solid sheet of vacuolated cells with clear cytoplasm and round and central nuclei. No atypia, lobular growth pattern, myxoid matrix, bone infiltration, nor necrosis was present. Adjacent preexisting trabeculae were thickened and sclerotic. In cases in which immunohistochemical stains were performed, both BNCT, chondroid chordoma, and conventional chordoma samples presented positive immunostaining for brachyury (Clone 3E4.2, ready to use (RTU), Merk Millipore), cytokeratins (Clone AE1/AE3, RTU, Agilent-Dako), S-100 protein (polyclonal, RTU, Agilent-Dako), and EMA (Clone E29, RTU, Agilent-Dako). The dedifferentiated tumoral component was in two of the cases and was negative for brachyury and cytokeratins. Cell proliferation index (Ki67 [clone MIB-1, RTU, Agilent-Dako]) was less than 1% in BNCT cases, approximately 5–10% in conventional chordomas and $< 20\%$ in the dedifferentiated ones.

Follow-up information was available in thirty-three cases. The mean follow-up was 17 years (P25 = 4, P75 = 32). Twelve conventional chordoma cases, the chondroid chordoma subtype case, the dedifferentiated chordomas, and a conventional chordoma with BNCT foci resulted in death-related disease. Seventeen cases were alive, including all the BNCT. Three conventional chordoma cases and one dedifferentiated chordoma developed distant metastasis to the liver or lungs. Fifteen conventional chordoma cases

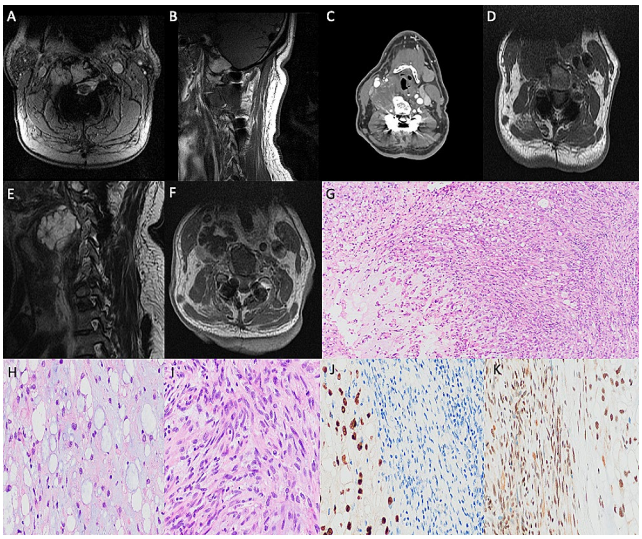

Fig. 6 Dedifferentiated chordoma. (**A**) Initial axial T2-WI and (**B**) Sagittal T1-WI: an expansive lesion hyperintense in T2 and isointense with the muscle in T1, located in the right hemibody and vertebral process of C2, which breaks the cortex and partially enters the spinal canal obliterating the right lateral subarachnoid space but without spinal cord involvement. It engulfs the vertebral artery without occluding it. Magnetic susceptibility artefacts produced by osteosynthesis material (previous arthrodesis). (**C**) Actual CT Axial image centered on C3 with intravenous contrast. There is a soft tissue mass in broad contact with the right hemi-body of C3, with poorly defined borders and a peripheral predominant enhancement. The vertebral artery is engulfed in the mass. The tumor produces a mass effect in the larynx and displaces anteriorly the carotid artery and the jugular vein. (**D**) Actual MRI Axial T1-weighted, (**E**) Sagittal T2-WI and (**F**) Axial T1-WI image with paramagnetic contrast of the cervical spine: large paravertebral mass broadly contacting the body of C3 without infiltrating it, isointense with the muscle in T1-weighted sequences and markedly hyperintense in T2. In this sequence the borders are hypointense and lobulated. Paramagnetic contrast shows heterogeneous and nodular enhancement in the periphery, suggesting central necrosis. (**G**) Transition between physaliphorous cells in a myxoid stroma into a densely cellular tumor with scanty stroma and physaliphorous cells. (**H**) Conventional component: Sheet of physaliphorous cells in a myxo-chondroid stroma (H&E, x200). (**I**) Dedifferentiated component: Spindle and round pleomorphic and atypical cells in a dense eosinophilic stroma. (**J**) Diffuse nuclear Brachyury positivity in the conventional component and negativity in the dedifferentiated component (x400). **K**. Diffuse nuclear INI1 positivity in both components (x400)

and the dedifferentiated chordomas presented local recurrence from four months to fifteen years following surgery. Both distant metastases and local recidive were treated with IMRT or proton therapy.

Discussion

We described the clinical, radiological, and histological findings as well as the management of fifty cases of NCDL. BNCT tend to appear in adults but cases have also been reported in children [1]. Chordomas appear in all ages but are more frequent in patients aged 50 to 70[1]. All our cases were diagnosed in adult patients with a mean age of 50 years. BNCT occur in the skull base, vertebral bodies, and sacrococcygeal spine [11]. All our cases of BNCT and chordoma with BNCT foci arose in the sacrum. Chordomas affect the axial skeleton, predominantly in the skull base and coccyx [1]. Our cases were more frequently located in the mobile vertebrae, followed by the sacrum and skull base. The chondroid chordomas arose in the skull base as is most reflected in medical literature [15]. BNCT are usually found incidentally on imaging, but they may present pain [12]. Two of our cases were incidentally detected but one patient referral was due to localized pain. Chordomas present pain and site-related neurological symptoms [7]. The two patients having BNCT with chordoma presented also lumbar pain. Most of our conventional chordoma cases debuted with neurological symptoms and pain except one case that was incidentally detected in radiological tests.

BNCT are most hidden in radiography. On CT, they appear as patchy sclerotic lesions having a trabecular architecture. They do not destroy cortical bone and do not expand into adjacent soft tissues. On MRI, they display homogeneous low signal intensity on T1-WI and homogeneous high signal intensity on T2-WI and they do not display contrast enhancement [8, 13]. In some cases, there may be T1 hyperintensity areas corresponding to fatty bone marrow [1]. If typical imaging findings are identified, some authors suggest that biopsy is unnecessary [11]. The radiological differential diagnosis includes sclerotic vertebral lesions, such as enostosis (bone island), hemangioma, intraosseous hibernoma, and metastasis [6]. Chordomas are lobular, septated, predominantly lytic, and destructive lesions, displaying prominent osseous expansile remodeling, which break cortical bone and invade adjacent soft tissues on CT [1]. In some sacral cases, sclerotic areas may be seen and they correspond to small punctate areas of amorphous calcification [14]. In vertebral chordomas, areas of bone sclerosis are more frequently detected than in the sacral region [14]. MRI reveals heterogeneously low signal intensity on T1-weighted imaging, heterogeneously high signal intensity on T2-weighted imaging, and variable contrast enhancement, usually mild to moderate, or marked less frequently [7, 14]. Radiological MRI chordoma findings reflect the high-water content in the myxoid matrix of these tumors. Hypointense areas may be seen in some cases, due to native entrapped bone trabeculae. Differential radiological diagnoses of clival chordomas are craniopharyngioma, giant pituitary macroadenoma, or metastasis [6, 14]. In sacral cases, it may be confused with plasmacytoma, lymphoma, chondrosarcoma, meningioma, or metastasis [6, 14]. In our two cases of chordoma with BNCT foci, the BNCT component was not radiologically detected. The most significant discriminators favoring the

diagnosis of BNCT in contradistinction to chordoma are sclerosis with maintenance of the trabecular architecture, no component of osseous or cortical bone destruction, absence of an associated extraosseous component, and the lack of contrast enhancement on MRI. Atypical imaging features of BNCT defined by Carter et al. [5] include evidence of significant contrast enhancement, minimal interval growth, bone lysis foci, and minimal soft tissue components. These cases require careful clinical and imaging follow-up. Chondroid chordomas are hypointense on T1-WI and hyperintense on T2-WI sequences, with variable post-contrast enhancement [15]. Dedifferentiated chordomas are isointense on T1-WI and hyperintense on ill-defined solid T2-WI masses [6].

BNCT are unique lesions but may be multiple [16]. Chordomas are also solitary lesions [1]. The BNCT pathogenesis is unknown [1]. Chordomas arising from BNCT has been described [6, 7, 16]. In our two cases of conventional chordoma with BNCT foci, no previous BNCT diagnosis was registered locally. The possibility of chordomas being derived from BNCT cannot be ruled out, or that of synchronous tumor presentation. BNCT are small (< 3.5 cm), well defined, lack lobular growth pattern and myxoid matrix. Are formed of solid sheets of vacuolated cells with clear cytoplasm and round and eccentric nuclei adjacent to normal bone marrow areas [8]. Chordomas are larger and more lobular tumors (> 5 cm) extending to adjacent structures. They are made up of physaliphorous cells arranged in cords and nests in an abundant extracellular myxoid matrix with variable degrees of atypia, pleomorphism, and mitosis [8]. Differential diagnosis must be carried out with chondrosarcoma, chordoid meningioma, metastatic carcinoma, and myoepithelial bone tumor [6]. The chondroid chordoma contains large areas of a matrix that is suggestive of that of cartilaginous tumors [17]. Dedifferentiated chordoma presents well demarcated high-grade areas and conventional areas; or a dedifferentiation in a site where previous conventional chordoma was present [4]. The expression of brachyury transcription factor is the hallmark of chordoma and it also appears in BNCT [18, 19]. BNCT and chordomas express brachyury, cytokeratin, vimentin, EMA, and variably S-100[1]. Brachyury may appear in other neoplasms such as non-small cell lung carcinomas [20]. Dedifferentiated chordoma may lose brachyury expression [1].

BNCT prognosis is excellent and it does not require surgical treatment [1]. BNCT cases in our series did not present local recurrence nor metastasis despite the observational follow-up. Malignant transformation to chordoma is rare [1, 7, 16]. The overall median survival time with chordomas is 7 years [1]. Surgery has been an effective and reliable treatment method for patients with spinal chordoma [3]. In lesions below S3, a partial posterior sacrectomy is performed. At the level proximal to S3, resection is performed either posteriorly or by double anterior and posterior approach [21]. Preservation of S1 whenever possible reduces morbidity and mortality. In the case of S1 or lumbosacral junction involvement, a complete sacrectomy is required, which is a highly demanding and morbid technique [21]. In cases where the sacrectomy affects S1 or over half of the S1 body, reconstruction of the lumbopelvic defect is performed [22]. In our cases, surgery had the objective of en-bloc resection with free margins. This was not always possible at the upper cervical level or in large tumors of the lumbosacral spine.

Chordomas are locally aggressive lesions having a propensity for metastasis late in their clinical course, and the most frequent metastatic sites are lung, bone, lymph nodes, and subcutaneous tissue [1]. Multimodal therapy targeting more than one pathway and concurrent use of adjuvant radiotherapy may be more effective than singular pathway targeting [23]. Except for dedifferentiated and poorly differentiated chordomas, most chordomas do not respond to conventional systemic chemotherapy [14]. Recent studies using proton beam therapy or charged particle radiotherapy have revealed higher rates of localized control with safe outcomes [24]. In our patients, complementary therapies to surgery have helped to reduce the presence of local recurrences, but despite this, up to 56% of them have developed local recurrences. The brachyury vaccine is a promising therapeutic strategy but more trials are needed to evaluate its safety and efficacy [25]. Cryoablation has been proposed for use in recurrent sacrococcygeal tumors [26]. There was no significant difference in the overall survival rate between chordomas located in the sacrum and in the vertebral column in our patients, similar to previous literature [3].

Elderly spinal chordoma patients (over 60 aged), larger tumor size, the performing of non-surgical therapy, and distant metastasis were all associated with poorer overall survival [3, 27]. A prognostic nomogram has recently been proposed to predict cancer-specific survival in patients with spinal chordoma [28]. Our series shows that chordomas are relatively radiologically and histopathologically homogeneous tumors, but with a highly heterogeneous response to current treatment (surgery with or without complementary therapies). Chordomas are tumors that originate in anatomical areas that demand complex surgical procedures and new complementary therapeutic methods must be keeping studied to reduce the high rate of local recurrence.

Some of the strengths of our study include a very large cohort and extensive data collection. One of the main study biases relates to its observational nature, with the resulting limitations. Some data were unavailable in medical reports. Another relevant limitation of our work relates to the fact that medical care of these tumors has improved

considerably over years and the present work includes cases dated 50 years ago.

Conclusion

Correct differential diagnosis is necessary for lesions derived from notochordal cells due to therapeutic and prognostic implications. Clinical, radiological, and histopathological data must be considered to ensure a proper diagnosis. A desirable en-bloc resection with free margins, adjuvant therapy mainly based on radiotherapy, and careful follow-up with radiological images should be performed in chordoma cases. New therapeutic options are being developed to improve the quality of life and survival rates of these patients.

Funding This research did not receive any specific grant from funding agencies in the public, commercial, or non-profit sectors.

Declarations

Conflict of interest The authors declare that they have no conflicts of interest.

References

1. Tirabosco R, O'Donnell P, Yamaguchi T (2020) Conventional chordoma. WHO classification of Tumours of Soft tissue and bone, 5th edn. Agency for Research on Cancer
2. Chauvel A, Taillat F, Gille O et al (2005) Giant vertebral notochordal rest: a new entity distinct from chordoma. Histopathology 47(6):646–649. https://doi.org/10.1111/j.1365-2559.2005.02168.x
3. Pan Y, Lu L, Chen J, Zhong Y, Dai Z (2018) Analysis of prognostic factors for survival in patients with primary spinal chordoma using the SEER Registry from 1973 to 2014. J Orthop Surg Res 13(1):76. https://doi.org/10.1186/s13018-018-0784-3
4. Tirabosco R, Mangham DC, Rosenberg AE et al (2008) Brachyury expression in extra-axial skeletal and soft tissue chordomas: a marker that distinguishes chordoma from mixed tumor/myoepithelioma/parachordoma in soft tissue. Am J Surg Pathol 32(4):572–580. https://doi.org/10.1097/PAS.0b013e31815b693a
5. Carter JM, Wenger DE, Rose PS, Inwards CY (2017) Atypical notochordal cell tumors: a Series of Notochordal-derived tumors that defy current classification schemes. Am J Surg Pathol 41(1):39–48. https://doi.org/10.1097/PAS.0000000000000766
6. Yamaguchi T, Imada H, Iida S, Szuhai K (2017) Notochordal tumors. Surg Pathol Clin 10(3):637–656. https://doi.org/10.1016/j.path.2017.04.008
7. Arain A, Hornicek FJ, Schwab JH, Chebib I, Damron TA (2017) Chordoma arising from benign multifocal notochordal tumors. Skeletal Radiol 46(12):1745–1752. https://doi.org/10.1007/s00256-017-2727-1
8. Kreshak J, Larousserie F, Picci P et al (2014) Difficulty distinguishing benign notochordal cell tumor from chordoma further suggests a link between them. Cancer Imaging 14(1):4. https://doi.org/10.1186/1470-7330-14-4
9. Lauer SR, Edgar MA, Gardner JM, Sebastian A, Weiss SW (2013) Soft tissue chordomas: a clinicopathologic analysis of 11 cases. Am J Surg Pathol 37(5):719–726. https://doi.org/10.1097/PAS.0b013e31827813e7
10. Kikuchi Y, Yamaguchi T, Kishi H et al (2011) Pulmonary tumor with notochordal differentiation: report of 2 cases suggestive of benign notochordal cell tumor of extraosseous origin. Am J Surg Pathol 35(8):1158–1164. https://doi.org/10.1097/PAS.0b013e318220e085
11. Tateda S, Hashimoto K, Aizawa T et al (2018) Diagnosis of benign notochordal cell tumor of the spine: is a biopsy necessary? Clin Case Rep 6(1):63–67. https://doi.org/10.1002/ccr3.1287
12. Terzi S, Mobarec S, Bandiera S et al (2012) Diagnosis and treatment of benign notochordal cell tumors of the spine: report of 3 cases and literature review. Spine (Phila Pa 1976) 37(21):E1356–1360. https://doi.org/10.1097/BRS.0b013e318266e7e6
13. Martínez Gamarra C, Bernabéu Taboada D, Pozo Kreilinger JJ, Tapia Viñé M (2018) Benign notochordal cell tumors. Radiologia (Engl Ed) 60(2):167–170. https://doi.org/10.1016/j.rx.2017.06.008
14. Murphey MD, Minn MJ, Contreras AL et al (2023) Imaging of spinal chordoma and benign notochordal cell tumor (BNCT) with radiologic pathologic correlation. Skeletal Radiol 52(3):349–363. https://doi.org/10.1007/s00256-022-04158-7
15. Erazo IS, Galvis CF, Aguirre LE, Iglesias R, Abarca LC (2018) Clival Chondroid Chordoma: a Case Report and Review of the literature. Cureus Published Online September 28. https://doi.org/10.7759/cureus.3381
16. Deshpande V, Nielsen GP, Rosenthal DI, Rosenberg AE (2007) Intraosseous benign notochord cell tumors (BNCT): further evidence supporting a relationship to chordoma. Am J Surg Pathol 31(10):1573–1577. https://doi.org/10.1097/PAS.0b013e31805c9967
17. Rosenberg AE, Bhan AK, Lee JM (1995) Chondroid chordoma. Am J Clin Pathol 104(4):484. https://doi.org/10.1093/ajcp/104.4.484a
18. Vujovic S, Henderson S, Presneau N et al (2006) Brachyury, a crucial regulator of notochordal development, is a novel biomarker for chordomas. J Pathol 209(2):157–165. https://doi.org/10.1002/path.1969
19. Presneau N, Shalaby A, Ye H et al (2011) Role of the transcription factor T (brachyury) in the pathogenesis of sporadic chordoma: a genetic and functional-based study. J Pathol 223(3):327–335. https://doi.org/10.1002/path.2816
20. Barresi V, Ieni A, Branca G, Tuccari G, Brachyury (2014) A diagnostic marker for the Differential diagnosis of Chordoma and Hemangioblastoma versus neoplastic histological mimickers. Dis Markers 2014:1–7. https://doi.org/10.1155/2014/514753
21. Court C, Briand S, Mir O et al (2022) Management of chordoma of the sacrum and mobile spine. Orthop Traumatol Surg Res 108(1S):103169. https://doi.org/10.1016/j.otsr.2021.103169
22. Bederman SS, Shah KN, Hassan JM, Hoang BH, Kiester PD, Bhatia NN (2014) Surgical techniques for spinopelvic reconstruction following total sacrectomy: a systematic review. Eur Spine J 23(2):305–319. https://doi.org/10.1007/s00586-013-3075-z
23. Akinduro OO, Suarez-Meade P, Garcia D et al (2021) Targeted therapy for Chordoma: Key Molecular Signaling pathways and the role of Multimodal Therapy. Targ Oncol 16(3):325–337. https://doi.org/10.1007/s11523-021-00814-5
24. Chhabra AM, Rice SR, Holtzman A et al (2023) Clinical outcomes and toxicities of 100 patients treated with proton therapy for chordoma on the Proton collaborative group prospective registry. Radiother Oncol 183:109551. https://doi.org/10.1016/j.radonc.2023.109551

25. Meng T, Jin J, Jiang C et al (2019) Molecular targeted therapy in the treatment of Chordoma: a systematic review. Front Oncol 9:30. https://doi.org/10.3389/fonc.2019.00030
26. Kurup AN, Woodrum DA, Morris JM et al (2012) Cryoablation of Recurrent Sacrococcygeal tumors. J Vasc Interv Radiol 23(8):1070–1075. https://doi.org/10.1016/j.jvir.2012.05.043
27. Lee IJ, Lee RJ, Fahim DK (2017) Prognostic factors and survival outcome in patients with Chordoma in the United States: a Population-based analysis. World Neurosurg 104:346–355. https://doi.org/10.1016/j.wneu.2017.04.118
28. Huang Z, Fan Z, Zhao C, Sun H (2021) A Novel Nomogram for Predicting Cancer-specific survival in patients with spinal chordoma: a Population-based analysis. Technol Cancer Res Treat 20:153303382110365. https://doi.org/10.1177/15330338211036533